

## **Design of buildings for wind and earthquake**

**\*Aly Mousaad Aly<sup>1)</sup>**

<sup>1)</sup> *Department of Civil Engineering, Louisiana State University, LA 70803, USA*  
<sup>1)</sup> [aly@LSU.edu](mailto:aly@LSU.edu)

### **ABSTRACT**

Buildings are usually subjected to static loads, such as, occupants' weight, equipment, furniture, and the weight of the structure. However, two important environmental loads that are different in nature may attack our buildings once or twice during their lifetime. The nature of the two loads are totally different from the static load, and even if they could be expressed as equivalent static loads, tall buildings and flexible structures may amplify the internal loads resulting in additional inertia loads which can alarm the serviceability and the comfort concern of people inside a building, or even lead to a complete collapse. When it comes to dynamics and load-structure interaction, the inherently low damping in buildings is a key parameter that can be used to control the behavior of a structure under such dynamic loads. In addition, building's orientation change can result into wind response/load reduction.

### **1. INTRODUCTION**

High-rise buildings are an increasingly common sight because they provide a high ratio of rentable floor space per unit area of land, in addition to other factors, such as architectural and energy perspectives. Tall buildings or 'skyscrapers' can be artificially lighted and the energy requirements can be covered by renewable energy or other electricity generation of low greenhouse gas emissions. Heating and cooling of skyscrapers can be efficient, because of centralized HVAC systems, heat radiation blocking windows and small surface area of the building. There is a Leadership in Energy and Environmental Design (LEED) certification for skyscrapers. For instance, the Empire State Building received a gold rating in September 2011 as the tallest LEED certified building in the United States (Bullard 2011). Also, the 30 St Mary Axe (the Gherkin) in London, the United Kingdom, is an environmentally friendly skyscraper (Frej and Browning 2005).

On the other hand, developments in structural materials and design technology in civil engineering have led to designs that satisfy strength requirements but are often very flexible. This flexibility can cause unfavorable vibrations when the structure is subjected to wind or earthquake loads. These vibrations may lead to serious structural damage and affect the comfort of the occupants. Dynamics of buildings greatly depends on the characteristics of the external excitation as well as the physical

---

<sup>1)</sup> Assistant Professor

properties of the building in terms of generalized masses, frequencies, and damping. Wind loads are characterized by low frequencies while earthquakes usually contain higher frequency load components. Fig. 1 shows general spectra of wind and earthquake loads. Most of the dynamics-associated damage and discomfort in buildings are referred to excitations close to first few modes. In super tall buildings, however, first modes are likely to have low frequencies which make them mostly affected by wind loads rather than earthquakes. On the opposite, short buildings are much suffered of dynamics-associated damage under earthquake loads which likely occurs at the dominant frequencies of these kinds of structures.

Extreme wind events compete with earthquakes as the dominant environmental design loading for structures. Both loads have caused catastrophic damages over the past years, although large damaging earthquakes have tended to occur less often than severe windstorms. On almost every day of the year a severe windstorm is happening somewhere on earth. Although many storms are small and localized, the most severe of all wind events, tropical cyclones, occurs over the tropical oceans then make land falling causing huge losses to life and properties.

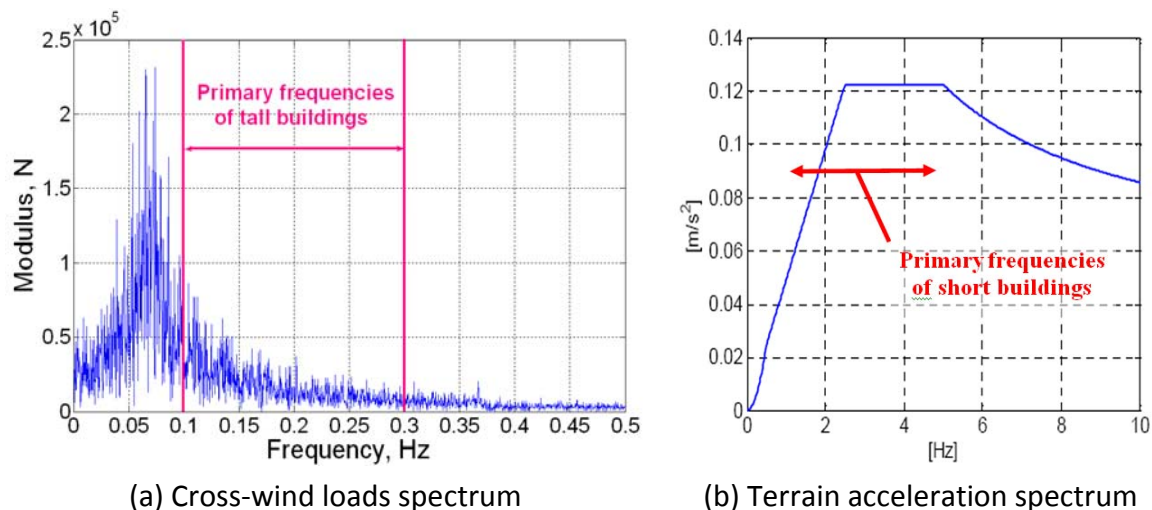


Fig. 1 Wind and earthquake general spectrums

### 1.1 Wind effects on buildings

Wind can be low, moderate, strong, and extremely destructive. While low and moderate winds are beneficial for pollution dispersion and electric power generation, strong and extreme wind events can cause devastating effects on the infrastructure. Extreme winds may cause damage to low-rise buildings in a form of windows damage, roof loss, or even complete collapse of wooden structures. In tall buildings, however, both cladding loads and the dynamics of the structure become a concern. High-rise buildings are amongst the more wind-sensitive structures. The lateral wind load imposed on super-tall structures is generally the governing factor in the structural design. It was inevitable that their response to wind would be of concern to structural engineers and attract the interest of early experimenters, both in the wind tunnel and in full-scale. Wind loads and the associated structural responses are a governing factor in the design of the steel framing system of many high-rise buildings. Wind load capacity

is also a key factor in determining the overall strength of towers. In addition, the design of high-rise buildings should take into account the comfort criteria due to the wind-induced vibration.

Wind-induced response/loading in structures depend on, among other factors, (1) terrain or mean wind velocity profile and turbulence characteristics (2) building's aerodynamic shape, (3) wind speed (which should not be always very high to cause damage – when Tacoma Narrows bridge failed it was moderate wind speed but negative aerodynamic damping or self-excitation existed (Billah and Scanlan 1991)), (4) wind direction, and (5) structural properties that may magnify wind loads at resonance. Not only the wind approaching buildings is a complex phenomenon, the flow pattern generated around buildings is complicated too. The flow pattern is distorted by the mean flow, flow separation, the formation of vortices, and development of the wake. Large wind pressure fluctuations due to these effects can occur on the surface of a building. As a result, large aerodynamic loads are imposed on the structural system and intense localized fluctuating forces act on the facade of such structures. Under the collective influence of these fluctuating forces, a building tends to vibrate in rectilinear and torsional modes (Mendis et al. 2007).

Along-wind loading and response of buildings due to buffeting can be assumed to consist of a mean component due to the action of the mean wind speed (the mean-hourly wind speed) and a fluctuating component. This is the basis of the so-called "gust-factor" approach, which is treated in many design codes. The mean load component is evaluated from the mean wind speed using pressure and load coefficients. The fluctuating loads are determined separately by a method which makes an allowance for the intensity of turbulence at the site, size reduction effects, and dynamic amplification (Davenport 1967). The dynamic response of buildings in the along-wind direction can be predicted with reasonable accuracy by the gust factor approach, provided the wind flow is not significantly affected by the presence of neighboring tall buildings or surrounding terrain.

Cross-wind oscillations can be very significant especially if the structural damping is small. The most common source of cross-wind excitation is that associated with 'vortex shedding' (Johns 1976, 1979). Tall buildings are bluff (as opposed to streamlined) bodies that cause the flow to separate from the surface of the structure, rather than follow the body contour (Fig. 2). The asymmetric pressure distribution, created by the vortices around the cross section, results in an alternating transverse force as these vortices are shed. If the structure is flexible, oscillations are transverse to the wind. The conditions for resonance would exist if the vortex shedding frequency coincides with the natural frequency of the structure. This situation can give rise to very large oscillations and possibly failure.

Fig. 3 presents plots among overall along-wind, cross-wind, torsional pressure loads obtained from wind tunnel testing of a tall building (Aly 2009). The target is to see if there are any correlations between any two of these load components. The figure shows that there is no correlation between the along-wind and the cross-wind loading. There is no correlation also between the along-wind and the torsional loads. However, the cross-wind and the torsional loads showed some correlations. The correlation between the cross-wind and the torsional loads depends on the geometry of the building. That is, the correlation is strong at incident angle of  $90^\circ$  while the two load

components are less correlated at wind incident of 180°.

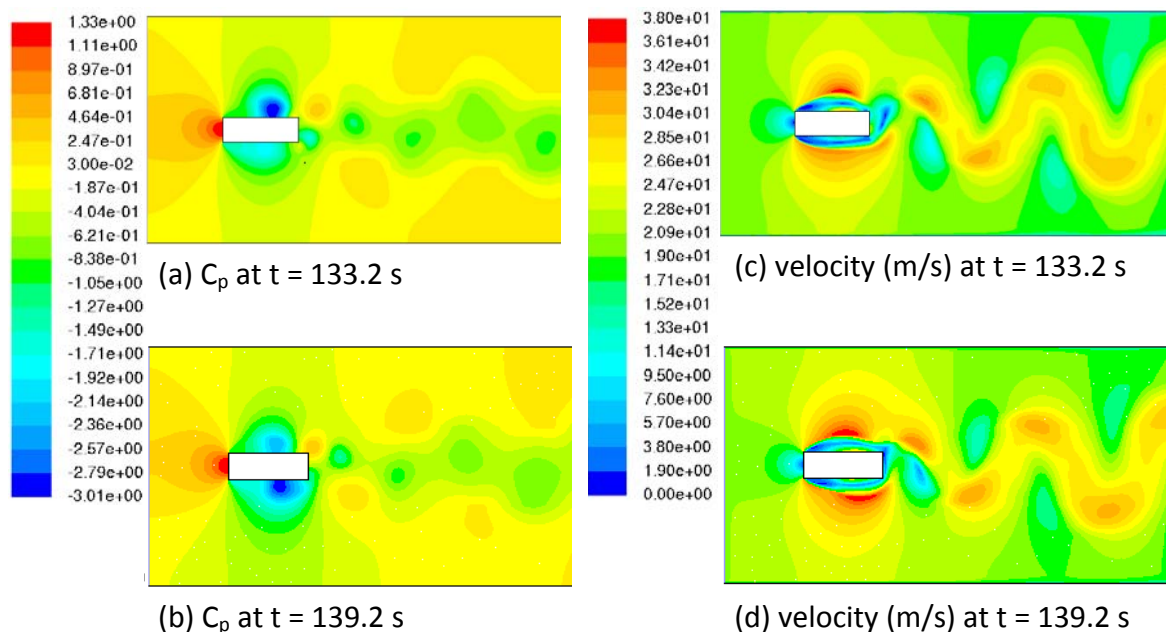


Fig. 2 Vortex shedding: (a) and (b) pressure coefficients at two different instants; (c) and (d) velocity contour at two time instants.

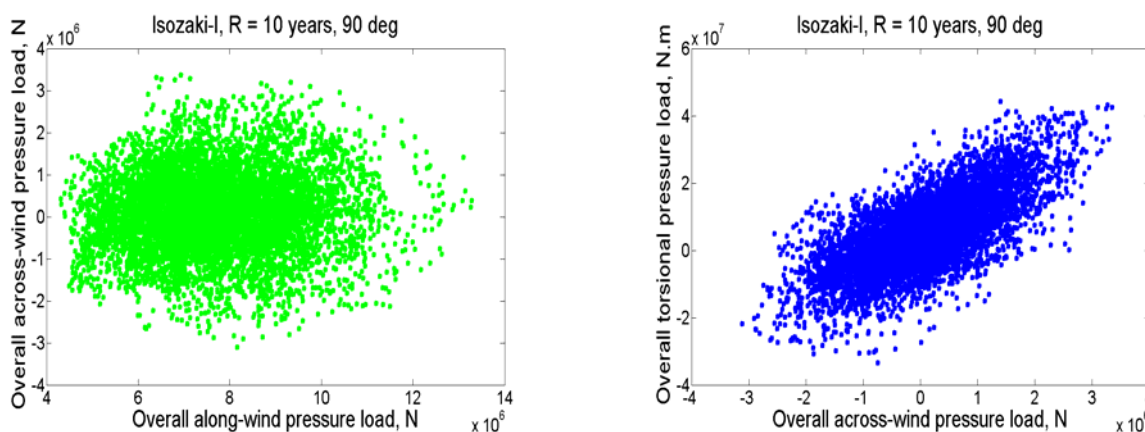


Fig. 3 Plots among different load components

Structural innovations and lightweight construction technology have reduced the stiffness, mass, and damping characteristics of modern buildings. In buildings experiencing wind motion problems, objects may vibrate, doors and chandeliers may swing, pictures may lean, and books may fall off shelves. If the building has a twisting action, its occupants may get an illusory sense that the world outside is moving, creating symptoms of vertigo and disorientation. In more violent storms, windows may break, creating safety problems for pedestrians below. Sometimes, strange and frightening noises are heard by the occupants as the wind shakes elevators, strains

floors and walls, and whistles around the sides.

Wind loading prediction A vital part of the design of modern tall buildings is the prediction of wind-induced motion and the assessment of its effects on occupant comfort. One of the primary purposes of wind engineering research is to predict wind-induced forces on structures. Wind-induced forces are dependent on structure shape, location on the structure, and the characteristics of wind (such as wind speed and angle of attack). Traditionally, wind loading on buildings can be evaluated analytically using some codes and formulas (ASCE 7-2010 2010; Eurocode 1 2004; Kareem 1992, 1998; Zhou et al. 2003). However, these standards provide little guidance for the critical cross-wind and torsional loading. This is partially attributed to the fact that the cross-wind and torsional responses, unlike the along-wind, result mainly from the aerodynamic pressure fluctuations in the separated shear layers and the wake flow fields, which have prevented, to date, any acceptable direct analytical relation to the oncoming velocity fluctuations (NatHaz 2008). Also, these methods have some limitations especially when some other tall structures exist in the vicinity of the building under consideration. Moreover, the evaluation process depends on many assumptions. To alleviate these problems, wind tunnel tests and full-scale measurement of wind are used to provide the more reliable wind loads on buildings.

Despite recent advancements in computational fluid dynamics, wind tunnel simulation of a scaled model is still the most common tool used to predict wind loading. Wind loads may be derived through multiple point synchronous scanning of pressures or by measured forces on the model mounted on a high frequency force balance (HFFB). High frequency force balance (HFFB) technique has been widely recognized for conveniently quantifying generalized wind forces on tall buildings (Kareem and Cermak 1979; Boggs and Peterka 1989). The generalized forces are then utilized for estimating building response with given structural characteristics. The HFFB technique generally requires mode shape corrections which are either based on empirical corrections, or analytical formulations derived on the basis of assumed wind loading models.

The integrated pressure modal load or IPML technique has the potential of addressing all of the limitations of the conventional high-frequency force-balance technique while still maintaining the same advantages that the technique has over the aeroelastic modeling (Aly 2013). Surface pressure measurement is favorable over force balance measurement as it gives the load distribution over the building surface and it cancels out the inertial effects (Zasso et al. 2008). The pressure integration technique can also be used to examine higher modes with non-monotonic mode shapes. The advantage of this technique is also that a single model used in a single testing session can produce both overall structural loads and cladding loads.

### *1.2 Earthquake effects on buildings*

When the ground shakes, buildings respond to the accelerations transmitted from the ground through the structure's foundation. The inertia of the building may cause shearing of the structure which can concentrate stresses on the weak walls or joints in the structure resulting in failure or perhaps total collapse. The type of shaking and the frequency of shaking depend on the structure. Tall buildings tend to amplify the motions

of longer periods when compared with small buildings. Taller buildings also tend to shake longer than short buildings, which can make them relatively more susceptible to damage. Fortunately many tall buildings are constructed to withstand strong winds and some precautions have been taken to reduce their tendency to shake. And they can be made resistant to earthquake vibrations (<http://eqseis.geosc.psu.edu> 2009).

Earthquake loading prediction Preparing structures (either new or old) for earthquakes is expensive and the level of investment is a social and political decision. The choice of building design is a compromise between appearances, function, structure, strength, and of course, cost. Standards are instituted through the establishment of Building Codes, which regulate the design and construction of buildings (ex. Eurocode 8 2003; ASCE 7-2010 2010). Most of the building codes are designed to protect first the building occupants, and second the building integrity. Building codes are usually drafted to meet the demands of the expected shaking in a given region that are summarized by seismologists and earthquake engineers in hazards maps. Hazard maps are constructed by examining

- The earthquake history of the region to estimate the probability of an earthquake
- The expected shaking intensity produced by the earthquake (often expressed as a peak acceleration)
- The frequency of the shaking, the distance from the fault
- The regional geology and site conditions

According to Koulouras et al. (2009), laboratory studies show that electromagnetic emissions in a wide frequency spectrum ranging from kilohertz (kHz) to very high megahertz (MHz) frequencies are produced by the opening of microcracks, with the MHz radiation appearing earlier than the kHz radiation. Since earthquakes are large-scale fracture phenomena in the Earth's heterogeneous crust, the radiated kHz–MHz electromagnetic emissions are detectable at a geological scale. A technique that uses the earth's electromagnetic emissions to predict earthquakes before its occurrence by a few days to a few hours before destructive earthquakes in Greece are discussed in Koulouras et al. (2009).

## **2. METHODOLOGY**

### *2.1 Description of the building*

The tower considered represents a high-rise building that is to be constructed in the city of Milan, Italy. The full-scale building has a height of 221.3 m above ground and a rectangular cross section of  $B/D = 2.56$  (B: chord length, D: thickness). The aspect ratio is about 9.3, which makes it sensitive to strong winds. The overall buildings mass is about  $1.4 \times 10^5$  ton. The structure has 50 stories above the ground level. The ground story has a height of 12.3 m, the successive stories have heights of 4.1 m and the last three stories have heights of 8.4 m, 4.2 m, 3.8 m respectively. There are four underground stories. Story -1 has a height of 7 m, story -2 has a height of 4 m, story -3 has a height of 5 m and story -4 has a height of 3 m. The building is designed for offices with restaurant at the last story. The building has two reinforced concrete cores that are able to carry all of the horizontal loads and part of the vertical loads. Beside the two vertical cores, the building has distributed vertical columns to carry the rest of the

vertical loads and a little portion of the horizontal loads. First six modes of the building are shown on Fig. 4. The modal parameters of the FEM for the first six modes are given in Table 1.

Table 1 Modal parameters of the FEM

Mode number	Generalized mass, (kg.m <sup>2</sup> )	Frequency, (Hz)
1	$3.55 \times 10^7$	0.1223
2	$3.13 \times 10^7$	0.1352
3	$3.27 \times 10^7$	0.4609
4	$3.27 \times 10^7$	0.6473
5	$2.08 \times 10^{10}$	1.0789
6	$4.50 \times 10^7$	1.0833

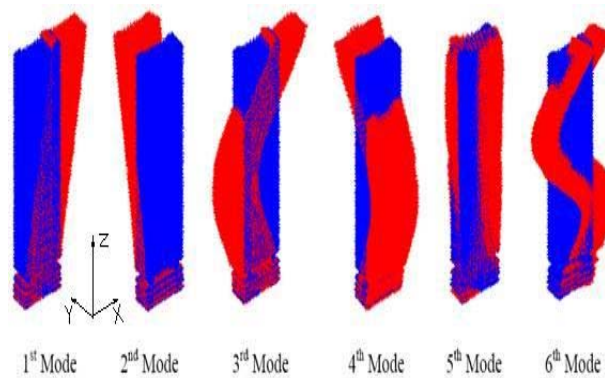


Fig. 4 Mode shapes of the FEM with the coordinate system

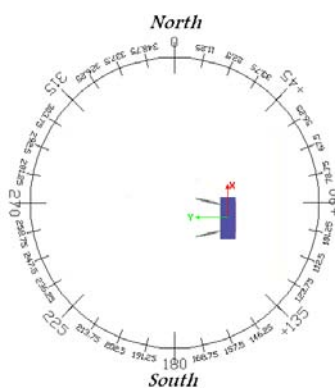


Fig. 5 Original orientations

Although finite element software packages can help to provide mode shapes, modal masses and modal frequencies of the desired modes, it does not provide information about damping in buildings. This is because unlike mass and rigidities that are distributed in a well-known manner along the elements, damping however is related to friction between joints and some hysteresis in the material which is difficult to be modeled. However, there is no convenient mean to refine the predictive capabilities regarding inherent structural damping, owing to its association with a number of complex mechanisms and even non-structural elements.

Full-scale measurement is considered to be the most reliable method for evaluating dynamic characteristics of buildings and structures. While the best way to get information about damping is to go on site and measure it, there have been some efforts to develop empirical predictive tools for damping estimation based on full-scale observations (Satake et al. 2003; Smith and Willford 2007). According to these measured data and for a reinforced concrete (RC) building with a height of about 240 m (including underground stories), the corresponding damping factor according to the lower trend line is about 0.6%.

Tamura and Yoshida (2008) presented a damping predictor for tall buildings that is dependent on the vibrations amplitude. The formula for reinforced concrete buildings is given by

$$\zeta = \frac{0.93}{H} + 470 \frac{x_H}{H} - 0.0018 \quad (1)$$

where  $\zeta$  is the first modal damping,  $x_H$  is the displacement at the top of the building, and  $H$  is the building's height. For  $x_H = 0.5$  m and overall building height of about 240 m the damping factor from Eq. (1) is about 1%. For  $x_H = 0.25$  m and 1 m the corresponding damping factors are .5% and 2% respectively. However, the damping factor for the Isozaki tower is assumed to be 1%.

## 2.2 Equation of motion

Equations of motion governing the behavior of the structure under wind loads are

$$\mathbf{M}\ddot{\mathbf{X}} + \mathbf{C}\dot{\mathbf{X}} + \mathbf{K}\mathbf{X} = \mathbf{F}(t) \quad (2)$$

where  $\mathbf{X} = [\mathbf{x} \ \mathbf{y} \ \mathbf{z}]^T$  is a  $3n \times 1$  vector and  $n$  is the number of nodes while  $\mathbf{x}$ ,  $\mathbf{y}$  and  $\mathbf{z}$  are vectors of nodal displacements in x, y, and z directions respectively.  $\mathbf{F}(t) = [\mathbf{F}_x(t) \ \mathbf{F}_y(t) \ \mathbf{F}_z(t)]^T$ , in which  $\mathbf{F}_x(t)$ ,  $\mathbf{F}_y(t)$ , and  $\mathbf{F}_z(t)$  are  $n \times 1$  vectors of external forces acting in x, y, and z directions respectively. Using the first six modes obtained by FEM (it was shown that there is no significant increase in the responses if modes higher than the sixth mode are considered for this specific structure), with the next transformation

$$\mathbf{X} = \Phi \mathbf{Q} \quad (3)$$

where  $\Phi$  is  $2n \times 6$  matrix of eigenvectors and  $\mathbf{Q}$  is  $6 \times 1$  vector of generalized displacements, i.e.

$$\Phi = \begin{bmatrix} \phi_1(x_1) & \phi_2(x_1) & \dots & \phi_6(x_1) \\ \phi_1(x_2) & \phi_2(x_2) & \dots & \phi_6(x_2) \\ \vdots & \vdots & & \vdots \\ \phi_1(x_n) & \phi_2(x_n) & \dots & \phi_6(x_n) \\ \phi_1(y_1) & \phi_2(y_1) & \dots & \phi_6(y_1) \\ \phi_1(y_2) & \phi_2(y_2) & \dots & \phi_6(y_2) \\ \vdots & \vdots & & \vdots \\ \phi_1(y_n) & \phi_2(y_n) & \dots & \phi_6(y_n) \\ \phi_1(z_1) & \phi_2(z_1) & \dots & \phi_6(z_1) \\ \phi_1(z_2) & \phi_2(z_2) & \dots & \phi_6(z_2) \\ \vdots & \vdots & & \vdots \\ \phi_1(z_n) & \phi_2(z_n) & \dots & \phi_6(z_n) \end{bmatrix}, \quad \mathbf{Q} = \begin{Bmatrix} q_1 \\ q_2 \\ \vdots \\ q_6 \end{Bmatrix} \quad (4)$$

Substituting by Eq. (3) into Eq. (2) and premultiplying by  $\Phi^T$ , one obtains

$$\Phi^T \mathbf{M} \Phi \ddot{\mathbf{Q}} + \Phi^T \mathbf{C} \Phi \dot{\mathbf{Q}} + \Phi^T \mathbf{K} \Phi \mathbf{Q} = \Phi^T \mathbf{F}(t) \quad (5)$$

By assuming the damping matrix,  $\mathbf{C}$ , to be proportional damping, Eq. (5) results into six uncoupled equations

$$\left. \begin{aligned} m_{11}\ddot{q}_1 + c_{11}\dot{q}_1 + k_{11}q_1 &= \sum_{i=1}^n \phi_1(x_i)F_{x,i}(t) + \sum_{i=1}^n \phi_1(y_i)F_{y,i}(t) + \sum_{i=1}^n \phi_1(z_i)F_{z,i}(t) = GF_1 \\ m_{22}\ddot{q}_2 + c_{22}\dot{q}_2 + k_{22}q_2 &= \sum_{i=1}^n \phi_2(x_i)F_{x,i}(t) + \sum_{i=1}^n \phi_2(y_i)F_{y,i}(t) + \sum_{i=1}^n \phi_2(z_i)F_{z,i}(t) = GF_2 \\ &\vdots \\ m_{66}\ddot{q}_6 + c_{66}\dot{q}_6 + k_{66}q_6 &= \sum_{i=1}^n \phi_6(x_i)F_{x,i}(t) + \sum_{i=1}^n \phi_6(y_i)F_{y,i}(t) + \sum_{i=1}^n \phi_6(z_i)F_{z,i}(t) = GF_6 \end{aligned} \right\} \quad (6)$$

where  $m_{ii}$ ,  $c_{ii}$ ,  $k_{ii}$ , and  $GF_i$  are generalized mass, generalized damping, generalized stiffness, and generalized force of the  $i^{\text{th}}$  mode respectively. The  $q_i(t)$  are then solved from each of the above equations. SIMULINK is used for the numerical solution of these equations (Attaway 2009).

### 3. RESPONSE UNDER WIND LOADING

The tower responses in the two lateral directions combined with the torsional responses (effect of higher modes on the responses is studied) are evaluated. Two important voids associated with procedures to aid in the design are considered: the first

is on the distributions of the wind loads; the second is on the effects of the mode shapes. Consideration of these two problems needs the wind tunnel tests and FEM.

### 3.1 Generalized forces

Using the measurements obtained by the pressure transducers, pressure coefficients (matrix  $\mathbf{C}_p$ ) are evaluated at each tap as a function of both space and time (Aly 2009; Aly 2013). These values are to be used with the full scale model to give the pressure distribution on the surface for different wind direction angles (Fig. 5). The pressure values on the surface of the full scale model can be calculated as follows

$$\mathbf{P}(space, time) = \frac{1}{2} \rho U^2 \mathbf{C}_p(space, time) \quad (7)$$

where  $\mathbf{P}(space, time)$  is a matrix containing the pressure values on the surface of the full scale model as a function of space ( $x$ ,  $y$ , and  $z$ ) and time,  $\rho$  is the air density which is assumed to be  $1.25 \text{ kg/m}^3$  (according to Eurocode 1 2004), and  $U$  is the mean wind speed that is dependent of the wind incident and the period of return.

The wind load at each node of the outer surface is the integration of the pressure over the surface area in the vicinity of the node as follows

$$\mathbf{F}(nodes, time) = \int \mathbf{P}(space, time) dA \quad (8)$$

As the time history of the pressures on the outer surfaces is calculated, the external forces acting on the nodes of the surface can be computed. The excitation forces acting on the internal nodes are of course equal to zero. The generalized forces are obtained as follows

$$\mathbf{GF} = \mathbf{F}^T \mathbf{F}(nodes, time) \quad (9)$$

Figs. 6-9 show the time history and the Fast Fourier Transform (FFT) of the generalized forces for the first two modes under wind incident angle of  $90^\circ$  and return 10 years for the configuration Isozaki-I (refer to Fig. 5 for the wind incident angle). The maximum values of the generalized forces are obtained as expected with the second mode. This is because the second mode of the building is a lateral vibration that coincides with the direction of the applied wind (the along wind loads are higher than the cross-wind loads for this specific angle due to the bigger drag surface). It is shown in the figure that the FFT of the generalized force of the second mode indicates that the forces with high amplitudes occur at lower frequencies than that of the first mode. This means that, unlike the along wind loads, cross-wind excitations occurs at higher frequencies than the along-wind which means that cross-wind fluctuating response may be higher than the along-wind response.

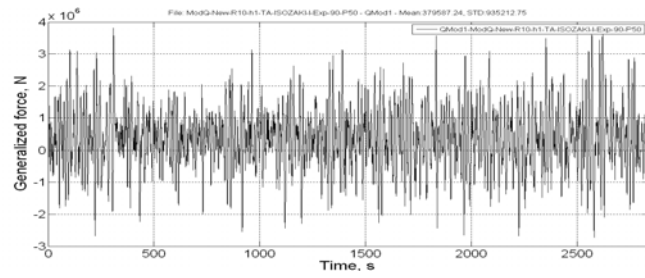


Fig. 6 Time history of the generalized force for incident angle of 90° (first mode)

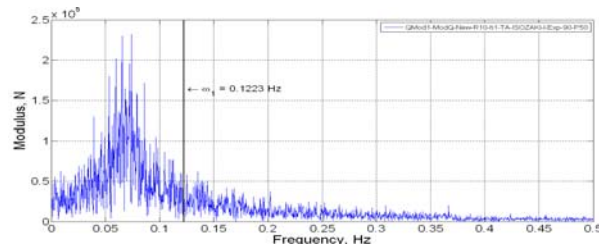


Fig. 7 FFT of the generalized force (first mode)

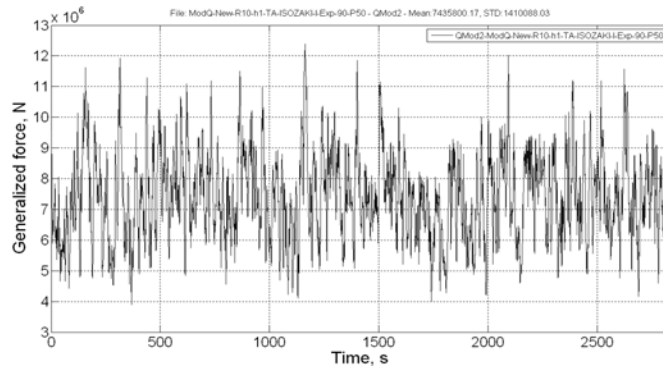


Fig. 8 Time history of the generalized force (second mode)

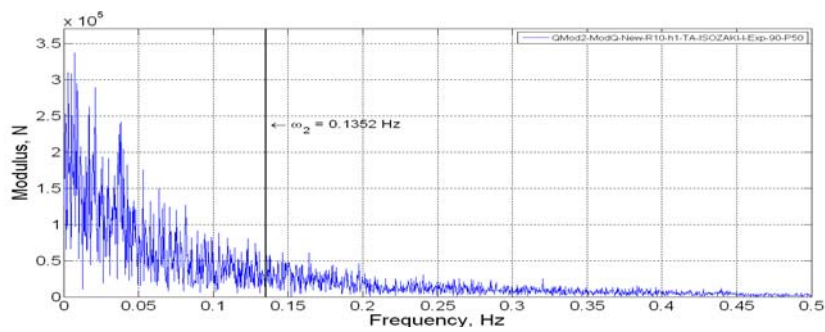


Fig. 9 FFT of the generalized force (second mode)

### 3.2 Response under wind

Once the generalized forces are obtained from Eq. (9), Eqs. (6) are numerically solved to have the generalized displacements then from Eq. (3) the real responses are obtained. Table 1 gives the response of the tower in the along-wind (y-direction) and the cross-wind (x-direction) directions for a wind incident of 90° with different considerations of the number of modes. It is shown that the displacement response of the building is dominated by the first two vibrational modes. However, the acceleration response is contributed not only by the first two lateral vibrational modes but also by higher modes (Table 2). The contributions of higher modes to the peak accelerations are about 10.6% and 12.8% in the x and y-directions respectively.

FFT of the displacement and acceleration responses of the top corner of the building are shown in Fig. 10 and Fig. 11. Again it is shown that the acceleration response is contributed not only by lower frequencies but also by higher frequencies (higher modes) while the displacement is dominant by lower frequencies.

Table 1 Displacement response of the top corner of the tower for an incident angle of 90°

Modes	rms disp., m		mean disp., m		peak disp., m	
	x	y	x	y	x	y
1	0.0631	0.0024	0.0087	0.0003	0.2460	0.0092
1:2	0.0632	0.0743	0.0032	0.1574	0.2424	0.4086
1:3	0.0629	0.0743	0.0031	0.1574	0.2428	0.4086
1:4	0.0629	0.0741	0.0031	0.1547	0.2428	0.4053
1:5	0.0629	0.0741	0.0031	0.1546	0.2428	0.4051
1:6	0.0629	0.0741	0.0031	0.1547	0.2427	0.4051

Table 2 Acceleration response of the top corner of the tower for an incident angle of 90°

modes	rms acc., milli-g		peak acc., milli-g	
	x	y	x	y
1	3.4845	0.1303	14.4055	0.5386
1:2	3.4935	4.8917	14.3285	18.7124
1:3	3.5332	4.8917	14.9738	18.7131
1:4	3.5332	4.9336	14.9720	20.7966
1:5	3.5349	4.9389	15.0110	21.0287
1:6	3.5421	4.9390	15.8521	21.1028

Table 3 Comparisons of the along-wind responses with codes

Results	ASCE	Eurocode	FEM
RMS disp., m	-	0.0939	0.0741
Peak disp., m	0.3747	0.4281	0.4051
RMS Acc., milli-g	4.8953	7.6730	4.9390
Peak Acc., milli-g	18.0241	24.2449	21.1028

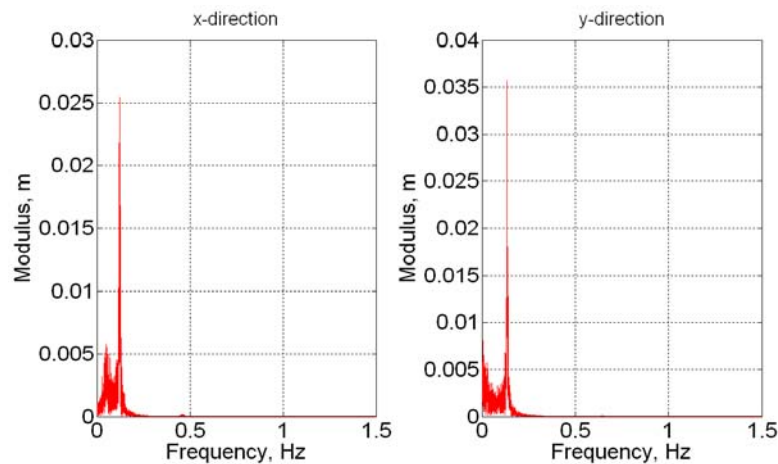


Fig. 10 FFT displacement of the top corner of the tower

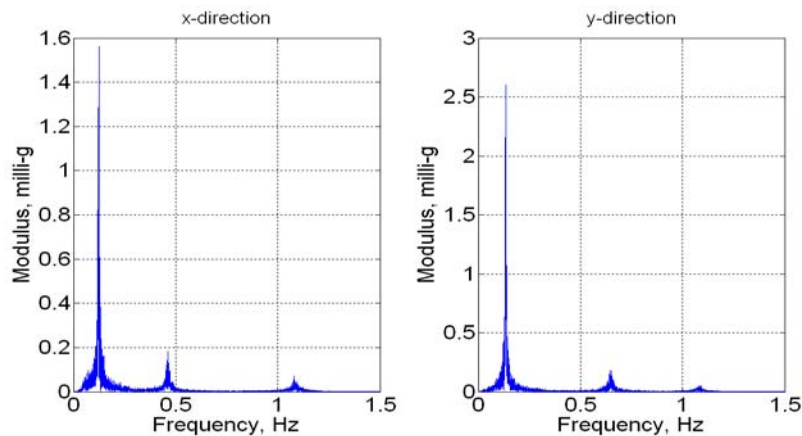


Fig. 11 FFT acceleration of the top corner of the tower

### 3.3 Comparison with codes

The American and the European standards (ASCE 7-2010 2010; Eurocode 1 2004) are used to obtain the along-wind responses of the tower assuming that the tower is almost a rectangular prism in its outer shape. For the American standard (ASCE 7-2010 2010), the basic wind speed is defined over a period of 3 seconds. To obtain the basic wind speed over a period of 3 seconds it is necessary to find the mean hourly

wind speed. The mean hourly wind speed is obtained using the formula (Simiu and Scanlan 1996, Eq. (2.3.37) of the book)

$$U_t(z) = U_{3600}(z) \left[ 1 + \frac{b^{1/2} \alpha(t)}{2.5 \ln(z/z_0)^{1/4}} \right] \quad (10)$$

The procedure followed to obtain the response of the building using the Eurocode is explained in Aly (2013).

Table 3 gives the along-wind displacement and acceleration responses obtained using ASCE 7-2010, Eurocode 1, and the proposed method (FEM) under wind incident angle of 90°. It is shown that there is some agreement between the results obtained using the two codes and the proposed method used in this study. However, the numerical technique used has the following advantages:

- It combines instantaneously the effects from along-wind, cross-wind, and torsion
- Higher modes can be considered (higher modes are important especially for acceleration)
- The maximum values of the responses may occur at angles other than 0° and 90°.
- At the same turbulence intensity, responses in the cross-wind direction may be larger than those in the along-wind direction. This reveals the importance of the technique proposed as many codes provide details to calculate the along-wind response but not the cross-wind and torsional responses.

The comfort criteria for this building is that the peak acceleration not to exceed 20 milli-g under wind with a return 10 years. This means that, if an acceleration peak factor of 3.5 is used, the RMS accelerations should not exceed 5.7 milli-g.

#### 3.4 Effects of wind incident and orientation on the responses

Due to the velocity unequal directionality and the effect of the wind attack angle, one can think about rotating the building. This may be possible if the building still in its preliminary design stages. Since the building is shown to be more sensitive to wind loads in the y-direction, the response of the building under wind that has the same mean speed (28.5 m/s) for all of the wind incident angles is first evaluated (Fig. 12 and Fig. 13).

From the previous results, one can see that the responses of the tower are the worst in the cross-wind of the y-direction (angle 180°). A good solution to such problem is to study the effect of the wind exposure angles (Fig. 13) on the response of the tower. The study showed that if the tower orientation is changed to be rotated clockwise, as shown on Fig. 14 (Suggested Orientation), the highest response in y-direction will be dramatically reduced. This is confirmed by Fig. 15. Among many possible orientations, the best orientation is shown to be the one at which the building is rotated 67.5°. Although this suggested orientation is favorable in reducing the responses in the y-direction, the response in the x-direction are increased. However, the increased response in the x-direction is lower than those in the y-direction under the original orientation. The reduction in the worst peak acceleration over the two directions (x and y) is shown to be more than 20%. This reduction is achieved without any additional cost to the building. This confirms the advantage of rotating the building to the suggested

orientation and reveals the importance of the response prediction in tall buildings during the preliminary design stages and before the real construction stage.

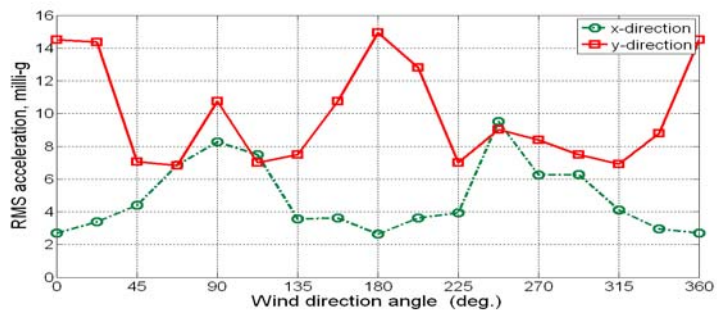


Fig. 12 RMS accelerations under the same mean wind speed

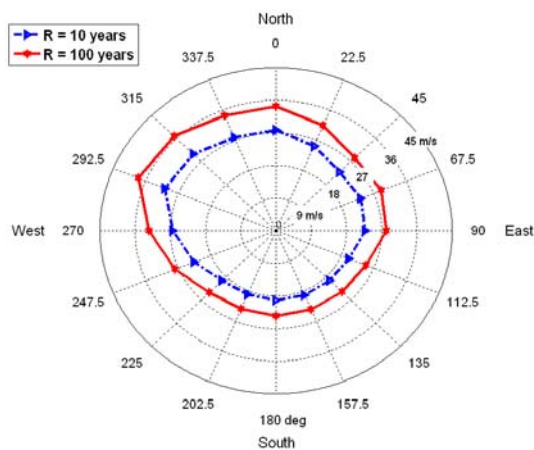
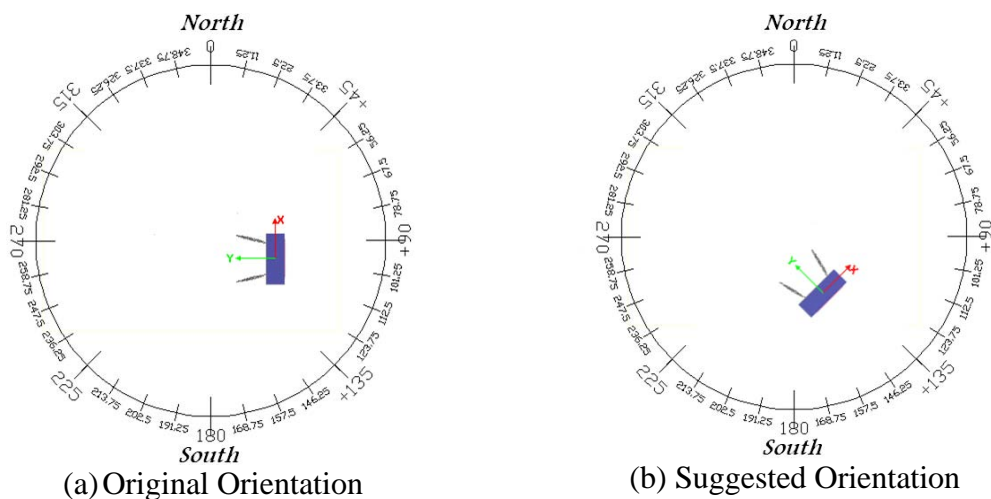


Fig. 13 Wind directionality for two return periods



(a) Original Orientation

(b) Suggested Orientation

Fig. 14 Original and suggested orientations

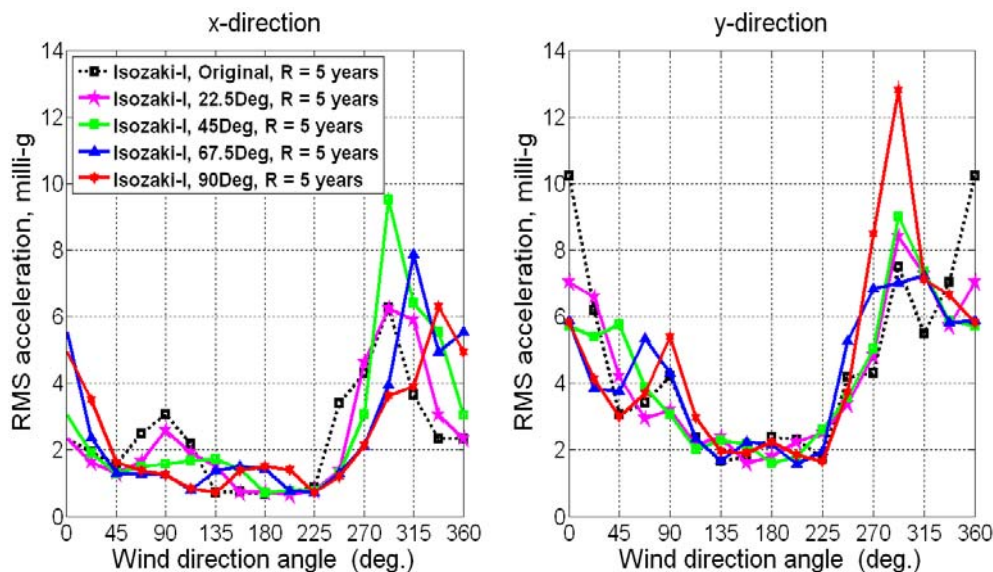


Fig. 15 Effect of changing orientation on the building's response

### 3.5 Aeroelastic response

In the previous section, the responses of the building were obtained numerically using wind tunnel data from a rigid model testing and FEM. Although this method is shown to be reasonable and have agreements with recent design codes, the method doesn't include the aerodynamic damping, which can be only obtained due to the interaction between the flow and the building. Such flow structure interaction requires the aeroelastic model experiment. This section gives an answer to an important question that is: is the aeroelastic model experiment important for such kind of structures?

The same rigid model was reused here again but it was elastically supported (see Fig. 16) and the mass is adjusted. Beside the geometry similarity (between model and prototype), the aeroelastic model requires the following similarities (ASCE 1999)

$$\text{Mass: } \lambda_M = \lambda_L^3 \lambda_{\rho_s} \quad (11)$$

$$\text{Velocity: } \lambda_V = U_m / U_p \quad (12)$$

$$\text{Frequency: } \lambda_f = \lambda_V / \lambda_L \quad (13)$$

$$\text{Damping: } \zeta_m = \zeta_p \quad (14)$$

For a length scale  $\lambda_L$  of 1:100 and the density scale,  $\lambda_{\rho_s}$ , of 1, the mass scale  $\lambda_M$ , is 1:10e6. Assuming the velocity scale defined in Eq. (12) to be 1:10, the frequency scale defined by Eq. (13) is 10:1. The steel bars at the base of the model (flexible support) are preliminary designed to give the required natural frequencies in the two directions then the distances between the bars ( $L_x$  and  $L_y$  on Fig. 16) are adjusted to give the

required natural frequencies experimentally. FFT analyser is used to check the natural frequencies. From the similarity conditions, steel bars and blocks are added inside the model to adjust the generalized masses to be  $35.5 \text{ kg.m}^2$  and  $31.3 \text{ kg.m}^2$  in the x and y directions respectively. The aeroelastic model has two frequencies of 1.22 Hz and 1.35 Hz in the x and y directions respectively. According to Eq. (14), the damping factor of the model is taken to be the same as the prototype, that is 1% in the two lateral directions. Additional Airpots (dampers) are added at the base of the model to adjust the modal damping (see Fig. 16). The overall damping of the model was calculated from the time decay of the response using the logarithmic decrement technique. The damping of the Airpots has been changed up and down until the required amount of damping to the model is reached.

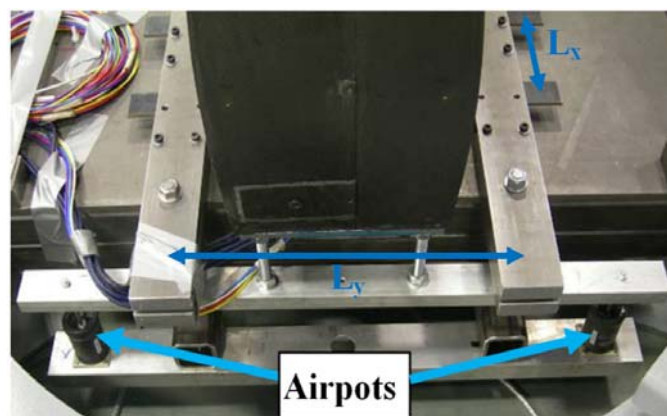


Fig. 16 Elastically supported model

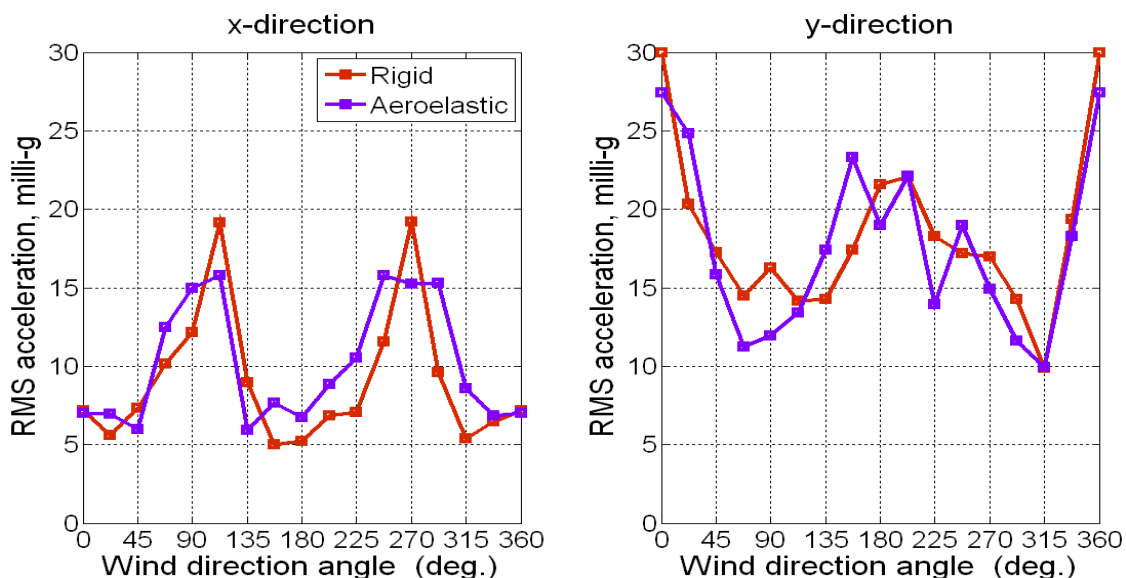


Fig. 17 Comparisons between accelerations for rigid and aeroelastic models

The building model is presented on the test table with the surrounding configuration "Isozaki-P11". That is the building with the other towers in the surrounding under the same wind profile. Three accelerometers are fixed near the top of the building model and at a height of 1.87 m from the base. One accelerometer is used in the x-direction (with a measuring range of  $\pm 3g$ ) while two other accelerometers are used in the y-direction (with a measuring range of  $\pm 20g$ ). The data of the accelerometers were acquired at a rate of 1000 Hz. An online FFT Analyser was used for direct monitoring of the measured data and to monitor the possible frequency change of the model during the test due to the flow structure interaction. Such phenomenon occurred and a coupling between the two modes was shown at a relatively high mean wind speed (about 8 m/s that corresponds to a prototype mean wind speed of 80 m/s). However, such mean wind speed is out of the predicted range of mean wind speeds at the site where the building (prototype) is to be constructed.

Since the building considered in the study has sharp-edged geometry, the results of the aeroelastic testing can be readily transformed to full scale without concerns about Reynolds number (ASCE 1999). The measured accelerations are fully representative to the prototype as the acceleration scale is 1:1. The acceleration measurements were filtered. The cut-off frequency used with the acceleration measurements is set to 10 Hz. This frequency is much more than five times the frequency of interest. Fig. 17 gives the acceleration response of the building under configuration "Isozaki-P11" and a prototype mean wind speed of about 38 m/s. The figure gives a comparison between the response obtained with the pressure integration technique and the measurements obtained from the aeroelastic model. One can see that there is a general agreement in the trend of the two methods. However the results cannot be precisely the same for the following reasons

- The wind flow presents a random phenomenon and it is difficult or even impossible to have the same results for the same test under the same configurations even if it is repeated several times.
- The fact that the damping produced by the Airpots (small precise pneumatic shock absorbers) and the structural part of the test model is nonlinear and may increase with the amplitude of oscillation.
- The contribution of the aerodynamic damping which may be positive or negative. However, the effect of the aerodynamic damping on the worst responses of the tower is shown to be positive which resulted into response reduction.
- The aeroelastic model used is a simple one that represents single degree of freedom in each lateral direction while the FEM considers much higher modes.
- The mode shapes of the test model are of course linear while those of the FEM have a second order trend.

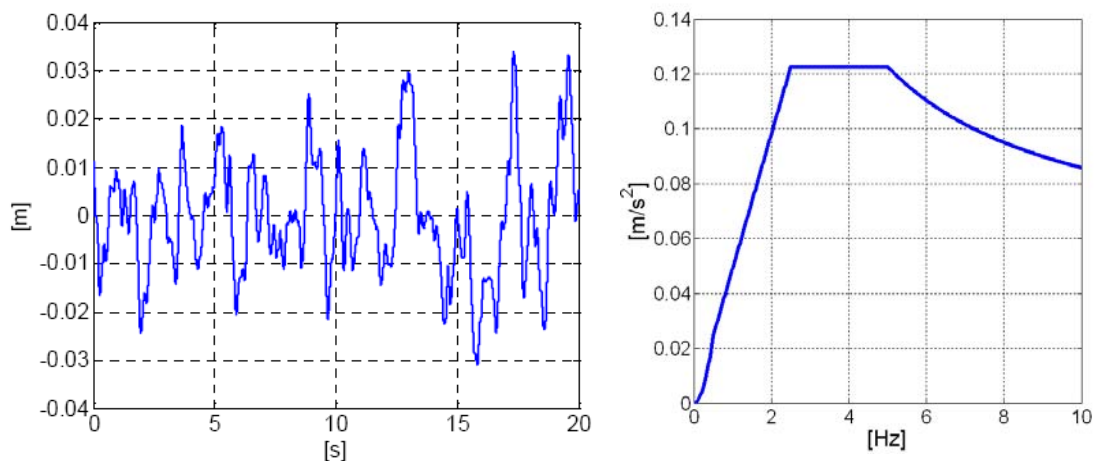
Since it was noticed for this building that there is a possibility of galloping under smooth flow (Zasso et al. 2008) for a wind attack angle of  $0^\circ$ , the aeroelastic experiment is conducted to verify the existence of this phenomenon. The aeroelastic instability occurred at a model mean wind speed of 1.94 m/s (19.4 m/s prototype) and a structural damping of 0.6%. However, the galloping instability was completely disappeared with higher damping (1%). Such conclusion should be taken into account for the design of similar structures in environments where low turbulence flow is expected.

General agreement between the results of the pressure integration technique and the aeroelastic experiment is shown. Keeping in mind the complexity and the time required to prepare the aeroelastic model (especially if the model is constructed to include higher modes with exact mode shapes) and to run the experiment (more expensive), the pressure integration technique with FEM is recommended for such kind of structures.

Aeroelastic wind tunnel experiment was presented. General agreements between the results of the pressure integration technique and the aeroelastic experiment are shown. However, the effect of the aerodynamic damping on the worst responses of the tower in the two lateral directions is shown to be positive which resulted into response reduction. Keeping in mind the complexity and the time required to prepare the aeroelastic model and to run the experiment, the pressure integration technique with FEM is recommended for such kind of structures. The advantage of the pressure integration technique is also that a single model used in a single testing session can produce both overall structural loads and cladding loads.

#### 4. RESPONSE UNDER EARTHQUAKE LOADING

Although earthquakes are shown to have major effects on short and medium-rise buildings (Aly 2005; Metwally et al. 2006; Aly and Christenson 2012), these effects may be lower on super tall buildings. To evaluate the effects of the earthquake on the tower, the time-history of the ground motion has been first evaluated according to the national standard of Italy (G.U. 2003) which defines the spectrum of the ground acceleration, as a function of both of the terrain characteristics and the typical stratigraphic profile of the site. The earthquake associated to the worst terrain type is taken. The spectrum of the ground acceleration and the corresponding time history of the ground motion are shown on Fig. 18.



(c) Time history of the ground motion

(d) Spectrum of the ground acceleration

Fig. 18 Time history and spectrum of the ground motion

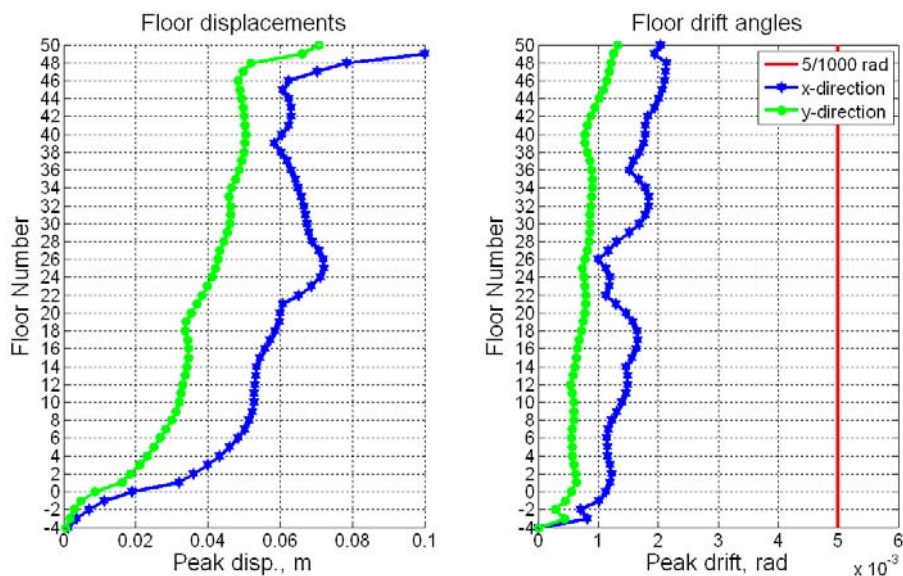


Fig. 19 Displacement and drift response of the tower under earthquake

Fig. 19 gives the peak displacements and the inter-story drift angles of the tower due to the earthquake ground motion. The inter-story drift angle is defined by

$$Drift\ angle = \frac{x_N - x_{N-1}}{\Delta H_N} \quad (15)$$

where  $x_N$  and  $x_{N-1}$  are the displacements of two successive floors and  $\Delta H_N$  is the height of the story number  $N$ . The horizontal component of the ground acceleration is assumed to attack the building in each of the two lateral directions alone. It is shown that the peak displacements of the tower due to earthquake in the two lateral directions are lower than the maximum peak displacements under wind. Furthermore, the inter-story drift angle is lower than the design value of 0.005.

## 5. MITIGATION TECHNIQUES

### 5.1 The role of damping

It was shown that the wind-induced responses of the tower are out of the comfort and security limits. This means that it is very important to produce damping in the building in order to reduce its response. Damping is the dissipation of energy from an oscillating system, primarily through friction. The kinetic energy is transformed into heat.

Although, finite element software packages can help to provide mode shapes, modal masses and modal frequencies of the desired modes, it does not provide information about damping in buildings. This is because unlike mass and rigidities that are distributed in a well-known matter along the elements, damping however is related to friction between joints and some hysteresis in the material which is difficult to be modeled. However, there is no convenient mean to refine the predictive capabilities regarding inherent structural damping, owing to its association with a number of complex mechanisms and even non-structural elements.

Unlike the uncertainty in the stiffness, uncertainty in structural damping is comparatively high. However, while the main objective of adding damping via specially engineered components is to reduce building motion and in some cases design loads, a good effect is that the uncertainty in damping level can also be reduced.

The main current of structural technology is about to change from conventional earthquake-resistant structures which are designed "not to collapse even under the strongest earthquake" to controlled structures which are intended "to suppress the vibration itself." The concept of employing structural control to minimize structural vibration was proposed in the 1970's (Yao 1972). Structural control is a diverse field of study. Structural control is one area of current research that looks promising in attaining reduce structural vibrations during loadings such as earthquakes and strong winds. Structural control based on various passive, active, hybrid and semi-active control schemes offers attractive opportunities to mitigate damage and loss of serviceability caused by natural hazards. The reducing of structural vibrations occurs by adding a mechanical system that is installed in a structure. The control of structural vibrations can also be done by various means such as modifying rigidities, masses, damping, or shape, and by providing passive or active counter forces (Housner et al. 1997). McNamara (1977) studied the tuned mass damper (TMD) as an energy-absorbing system to reduce wind-induced structural response of buildings in the elastic range of behavior. Active control techniques are studied intensively for the control of the response of tall buildings under wind loads (Soong 1990; Facioni et al. 1995; Gu and Peng 2002; Wu and Pan 2002; Lu et al. 2003). The most commonly used active control device for civil engineering structures is the active tuned mass damper (ATMD).

### *5.2 Robust tuned mass dampers*

Tuned mass dampers (TMDs) are used in both x and y directions. Although the mass of the TMD in the y-direction is taken as 3% of the first modal mass, it is still unable to satisfy the comfort criteria required. To overcome on this problem, an actuator is added to the TMD to form an active tuned mass damper (ATMD). ATMD is used in the y-direction in order to improve the performance and the robustness of the TMD. Both LQG and Fuzzy Logic controllers are used to provide the optimal control force for the ATMD. Robustness and effectiveness of the Fuzzy Logic controller over the LQG controller will be addressed.

The aim of the study presented in Aly (2014) and Aly et al. (2011a) was to control the responses of the high-rise building under the wind loads measured in the wind tunnel using both TMDs and ATMDs. Active control of the structure using LQG and fuzzy logic controllers under wind that is attacking from different directions is studied. Lateral responses of the building in the two directions are controlled simultaneously while the effect of the uncontrolled torsional responses of the structure is considered instantaneously. A good reduction in the response of the building is obtained with both TMDs and ATMDs. Fuzzy logic controller has proved its robustness and the requirement of lower control forces over the LQG controller.

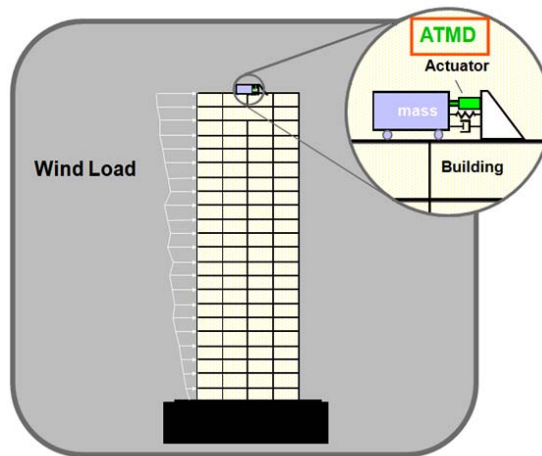


Fig. 20 Active tuned mass damper (ATMD)

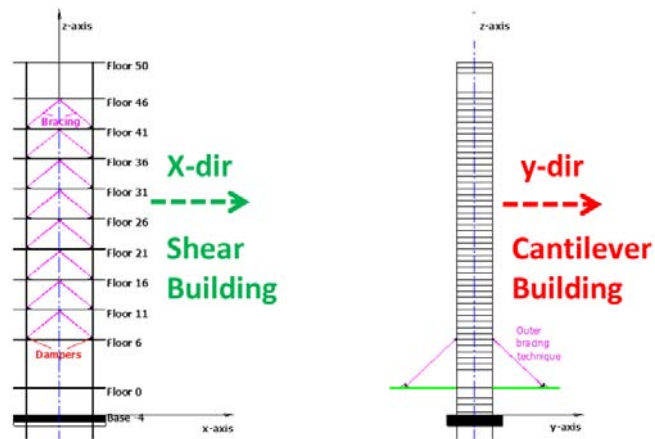


Fig. 21 Proposed configuration of the MR dampers with bracing system

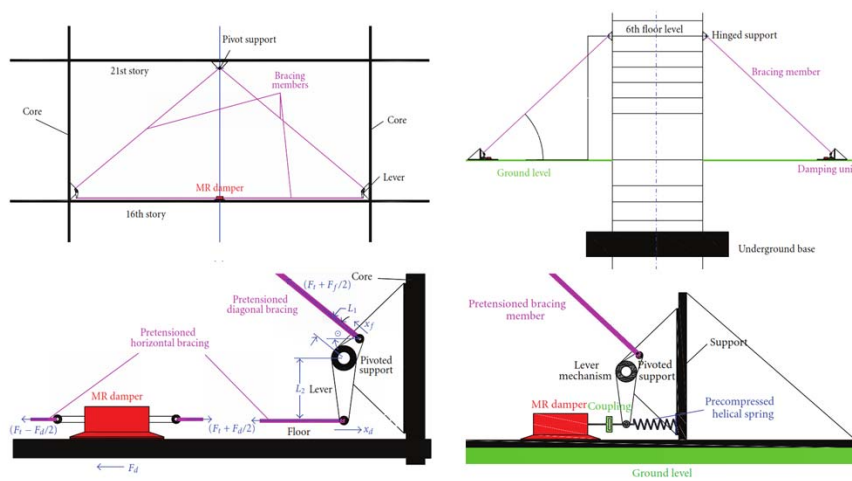


Fig. 22 Details of the MR damper lever mechanism bracing system

### *5.3 Magneto-rheological fluid dampers*

In recent years magnetorheological (MR) dampers have been verified with the unique ability to create the resisting force following the change of various characteristics. In Aly et al. (2011b, 2011c), MR dampers are placed in the tower as an alternative to TMDs and ATMD to reduce the wind-induced responses. The challenge in using such devices in tall buildings is related to where to put the device in the building. Unlike short and shear buildings, in which floor rotational angles are very small and there is a significant inter-story drift under dynamic loads, slender tall buildings, however, may behave like a cantilever. Cantilever like behavior of buildings makes it very difficult to have an effective internal bracing system. The building under consideration is shown to behave in one lateral direction like shear buildings (x-direction) and in the other direction as cantilever structures (y-direction). For the x-direction, internal bracings with MR dampers are used while for the y-direction outer bracings with MR dampers are proposed. Since the displacement across the damper is shown to be small, a lever mechanism is proposed for motions magnification. Both passive-on and decentralized bang-bang controllers showed that MR dampers with the proposed lever mechanism are effective in reducing the responses of the tower under wind loads in the two lateral directions.

Although TMDs and ATMD are shown to be effective in the response reduction of tall buildings under wind loads, they are large, heavy, and take up valuable space at the top of the building. Moreover, they are an additional cost to the project (see Fig. 20).

Viscous dampers and semiactive dampers can be used as alternatives to overcome on these problems. These devices do not require frequency tuning, and while there is an optimum resistance characteristic for each application, the overall damping achieved is usually not very sensitive to the exact resistance characteristic of the device (Smith and Willford 2007). It is therefore sometimes possible to damp several modes with one device. Magnetorheological dampers were used to reduce the accelerations and the design loads of the tower in the two lateral directions (Aly et al. 2011b, 2011c, see Fig. 21 and Fig. 22).

## **6. DISCUSSION**

In the last two centuries, some major structural failures due to winds have occurred. Large structures have experienced failures as well – for example, the collapse of the Ferry bridge cooling towers in the U.K. in 1965, and the permanent deformation of the columns of the Great Plains Life Building in Lubbock, Texas, during a tornado (1970). Moreover, many super tall buildings have seen to suffer from wind loads leading to structural annoying vibrations that cause, some time, horrible effects on the occupants. Such phenomenon needs a deep understanding in order to allow for providing adequate solutions.

Structural response prediction and reduction form an integral part of the building design process, providing architects and design engineers with a comprehensive understanding of the interaction between environmental factors and building design. A proper connotation of this interaction can provide significant cost savings to building owners in terms of developmental, material, and operational costs. To expose them to

the methods and procedures for the efficient application of wind studies in designing a building more economically than a similar building designed with more conservative building code provisions.

By so doing, the dynamic response of the building to wind effects (buffeting and vortex shedding) is virtually eliminated; leading to substantially reduced lateral design forces and assured occupant comfort. Substantial reductions in structural member size and construction cost savings can be realized in many cases. This may significantly improve the economic viability and sustainability of a development.

## **7. CONCLUSIONS**

The objective of the current paper was to further the understanding of wind and earthquake effects on high-rise buildings in order to apply such knowledge to the design of such structures. A reduction in the worst peak acceleration is shown to be more than 20%, by changing the building orientation. This reduction is achieved without any additional cost to the building which confirms the advantage of rotating the building to a suggested orientation and also shows the importance of the response prediction in tall buildings during the preliminary design stages and before the real construction stage. In addition, for the response prediction under wind loads, general agreements between the results of the pressure integration technique and the aeroelastic experiment exist. However, the effect of the aerodynamic damping on the worst responses of the tower in the two lateral directions is shown to be positive which resulted into response reduction. Keeping in mind the complexity and the time required to prepare the aeroelastic model and to run the experiment, the pressure integration technique with FEM is recommended for such type of structure. The advantage of the pressure integration technique is also that a single model used in a single testing session can produce both overall structural loads and cladding loads. The study shows that wind and earthquake loads are different from each other and are also different from static loads. This comes from the spectral comparison of the response of the building under the two types of excitation. Earthquakes excite higher modes that produce less inter-story drift but higher accelerations which occurs for short time. Although the acceleration under wind are lower than that under earthquake, they occur for longer period which becomes a comfort issue. However, the drift under wind is larger which raises security issues. The results also show that tall buildings designed for wind may be safe under moderate earthquake loads. Appropriate damping techniques were brought for response reduction under wind loads.

## **ACKNOWLEDGEMENTS**

The experimental part in this paper was carried out at the wind tunnel of Politecnico di Milano (PoliMI). The help offered by many volunteers is really appreciated. The author would like to acknowledge the support he received from the PoliMI. Many thanks to Professor Alberto Zasso and the wind tunnel's research team for their help.

## REFERENCES

- Aly, A. M. (2009). On the Dynamics of Buildings Under Winds and Earthquakes: Response Prediction and Reduction. Ph.D. Dissertation, Department of Mechanical Engineering, Politecnico di Milano, Milan, Italy.
- Aly, A.M. (2014), "Proposed robust tuned mass damper for response mitigation in buildings exposed to multidirectional wind," *Struct. Des. Tall Spec. Build.*, **23**(9), 664–691.
- Aly, A.M., (2013), "Pressure Integration Technique for Predicting Wind-Induced Response of a High-Rise Building," *Alexandria Engineering Journal*, **52**(4), 717-731.
- Aly, A.M., Zasso, A. and Resta, F. (2011a), "Dynamics and control of high-rise buildings under multidirectional wind loads," *Smart Materials Research*, 549621, (15pp).
- Aly, A.M., Zasso, A. and Resta, F. (2011b), "On the dynamics of a very slender building under winds: response reduction using MR dampers with lever mechanism," *Struct. Des. Tall Spec. Build.*, **20**(5), 541-553.
- Aly, A.M., Zasso, A. and Resta, F. (2011c), "Proposed configurations for the use of smart dampers with bracings in tall buildings," *Smart Materials Research*, Article ID 251543, 16 pages.
- Aly, A.M. (2005). Vibration control in structures due to earthquake effects using MR damper. M.Sc. Thesis, Department of Mechanical Engineering, Alexandria University.
- ASCE 7-2010, (2010). Minimum design loads for buildings and other structures, ASCE Standard, ASCE/SEI 7-10, American Society of Civil Engineers, Reston, Virginia.
- ASCE, (1999). Wind Tunnel Studies of Buildings and Structures. ASCE Manuals and Reports of Engineering Practice No. 67, American Society of Civil Engineers, Virginia.
- Attaway, Matlab: A Practical Introduction to Programming and Problem Solving, Butterworth-Heinemann, Amsterdam, The Netherlands, 2009.
- Billah, K.Y. and Scanlan, R.H. (1991), "Resonance, Tacoma Narrows bridge failure, and undergraduate physics textbooks," *Am. J. Phys.*, **59**(2), 118-124.
- Boggs, D.W. and Peterka, J.A. (1989), "Aerodynamic model tests of tall buildings," *J. Eng. Mech.*, **115**(3), 618–635.
- Bullard, L. (2011). The Empire State Building. Lerner Publications.
- Davenport, A.G. (1967), "The dependence of wind loads on meteorological parameters," *Proc. Int. Res. Seminar, Wind Effects on Buildings and Structures*, Ottawa, Univ. of Toronto Press, 19-82.
- Eurocode 1, 2004. Actions on structures - Part 1-4: General actions - Wind actions. prEN 1991-1-4, European Standard.
- Eurocode 8. (2003). Design of structures for earthquake resistance - Part 1: General rules, seismic actions and rules for buildings. prEN 1998-1, European Standard.
- Facioni, R.J., Kwok, K.C.S. and Samali, B. (1995), "Wind tunnel investigation of active vibration control of tall buildings," *J. Wind Eng. Ind. Aerodyn.*, (54-55), 397-412.
- Frej, A., Browning, W.D. 2005. Green Office Buildings: A Practical Guide to Development. Urban Land Institute.

- G.U. (2003). Supplemento n. 72 della Gazzetta Ufficiale n. 105 del 08.05.2003 (in Italian).
- Gu, M. and Peng, F. (2002), "An experimental study of active control of wind-induced vibration of super-tall buildings," *J. Wind Eng. Ind. Aerodyn.*, **90**, 1919-1931.
- Housner, G.W., Bergman, L.A., Caughey, T.K, Chassiakos, A.G., Claus, R.O., Masri, S.F., Skelton, R.E., Soong, T.T., Spencer, B.F. and Yao, J.T.P. (1997), "Structural control: Past, present, and future," *J. Eng. Mech., ASCE*, **123**(9), 897-971.
- Johns, D.J. (1976), "Wind Excited Behavior of Structures," *The Shock and Vibration Digest* **8**(4), 67-75.
- Johns, D.J. (1979), "Wind Excited Behavior of Structures II," *The Shock and Vibration Digest*, **11**(4), 17-29.
- Kareem, A. (1992), "Dynamic Response of High-Rise Buildings to Stochastic Wind Loads," *J. Wind Eng. Ind. Aerodyn.*, **42**(1-3), 1101-1112.
- Kareem, A. (1998), "Aerodynamic Response of Structures with Parametric Uncertainties," *Struct. Safety*, **5**(3), 205-225.
- Kareem, A., and Cermak, J. E. (1979), "Wind tunnel simulation of wind structure interactions," *ISA Trans.*, **18**(4), 23-41.
- Koulouras, G., Balasis, G., Kiourktsidis, I., Nannos, E., Kontakos, K., Stonham, J., Ruzhin, Y., Eftaxias, K., Cavouras, D. and Nomicos, C. (2009), "Discrimination between pre-seismic electromagnetic anomalies and solar activity effects," *Smart Mat. Struct.*, **79**(4), art. no. 045901.
- Lu, L.T., Chiang, W.L., Tang, J.P., Liu, M.Y. and Chen, C.W. (2003), "Active control for a benchmark building under wind excitations," *J. Wind Eng. Ind. Aerodyn.*, **91**(4), 469-493.
- McNamara, R.J. (1977), "Tuned Mass Dampers for Buildings," *J. Struct. Divis., ASCE*, **103**(9), 1785-1798.
- Mendis, P., Ngo, T., Haritos, N., Hira, A., Samali, B. and Cheung, J. (2007), "Wind Loading on Tall Buildings," *EJSE Special Issue: Loading on Structures*.
- Metwally, H.M., El-Souhily, B.M. and Aly, A. (2006), "Reducing vibration effects on buildings due to earthquake using magneto-rheological dampers," *Alex. Eng. J.*, **45**(2), 131-140.
- NatHaz. (2008), Aerodynamic Loads Database, <http://aerodata.ce.nd.edu/>.
- Satake N, Suda K, Arakawa T, Sasaki A and Tamura Y. (2003), "Damping evaluation Using Full-Scale Data of Building in Japan," *J. Struct. Eng., ASCE*, **129**, 470-477.
- Simiu, E. and Scanlan, R.H. (1996), *Wind Effects on Structures: Fundamentals and Applications to Design*, John Wiley & Sons, Inc., New York.
- Smith, R.J. and Willford, M.R. (2007), "The damped outrigger concept for tall buildings," *Struct. Des. Tall Spec. Build.*, **16**, 501-517.
- Soong, T.T. (1990). *Active Structural Control. Theory and Practice*. Longman.
- Tamura, Y. and Yoshida, A. (2008), "Amplitude Dependency of Damping in Buildings," 18th Analysis and Computation Specialty Conference, Vancouver, Canada.
- Wu, J.C. and Pan, B.C. (2002), "Wind tunnel verification of actively controlled high-rise building in along-wind motion," *J. Wind Eng. Ind. Aerodyn.*, **90**(12-15), 1933-1950.
- Yao, J.T.P. (1972), "Concept of Structural Control," *J. Struct. Divis., ASCE*, **98**(7), 1567-1574.

- Zasso, A., Aly, A.M., Rosa L. and Tomasini, G. "Wind induced dynamics of a prismatic slender building with 1:3 rectangular section," BBAA VI International Colloquium on Bluff Bodies Aerodynamics & Applications, Milano, Italy, 20-24 July 2008.
- Zhou, Y., Kijewski, T. and Kareem, A. (2003), "Aerodynamic loads on tall buildings: interactive database," J. Struct. Eng., **129**(3), 394-404.